Optimal design of photovoltaic shading systems for multi-story buildings

Li, X., Peng, J., Li, N., Wu, Y., Fang, Y., Li, T., Wang, M. & Wang, C.

Original citation & hyperlink:
Li, X, Peng, J, Li, N, Wu, Y, Fang, Y, Li, T, Wang, M & Wang, C 2019, 'Optimal design of photovoltaic shading systems for multi-story buildings' Journal of Cleaner Production, vol. (In-press), pp. (In-press).
https://dx.doi.org/10.1016/j.jclepro.2019.01.246

DOI 10.1016/j.jclepro.2019.01.246
ISSN 0959-6526
ESSN 1879-1786

Publisher: Elsevier

Accepted Manuscript

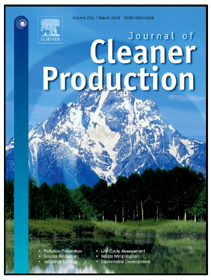

Optimal design of photovoltaic shading systems for multi-story buildings

Xue Li, Jinqing Peng, Nianping Li, Yupeng Wu, Yueping Fang, Tao Li, Meng Wang, Chunlei Wang

PII:	S0959-6526(19)30271-9
DOI:	10.1016/j.jclepro.2019.01.246
Reference:	JCLP 15633
To appear in:	*Journal of Cleaner Production*
Received Date:	17 September 2018
Accepted Date:	22 January 2019

Please cite this article as: Xue Li, Jinqing Peng, Nianping Li, Yupeng Wu, Yueping Fang, Tao Li, Meng Wang, Chunlei Wang, Optimal design of photovoltaic shading systems for multi-story buildings, *Journal of Cleaner Production* (2019), doi: 10.1016/j.jclepro.2019.01.246

Highlights:

1. This paper focuses on the optimal design of photovoltaic shading systems;
2. A special PV module configuration was presented to reduce shading effect;
3. Numerical model embodying a profile angle was developed to analyze shading effect;
4. Optimum tilt angles and widths were obtained by analyzing benefit per capacity.

Optimal design of photovoltaic shading systems for multi-story buildings

Xue Li[a,b], Jinqing Peng[a,b*], Nianping Li[a,b], Yupeng Wu[c], Yueping Fang[d], Tao Li[e], Meng Wang[a,b], Chunlei Wang[a,b]

[a] Key Laboratory of Building Safety and Energy Efficiency of the Ministry of Education, Hunan University, Changsha 410082, China

[b] College of Civil Engineering, Hunan University, Changsha 410081, China

[c] Department of the Architecture and Built Environment, Faculty of Engineering, University of Nottingham, Nottingham NG7 2RD, UK

[d] School of Energy, Construction and Environment, Coventry University, Coventry CV1 5FB, UK

[e] School of Physics and Electrical Engineering, Qinghai Normal University, Xining, 810008, China

*Corresponding author E-mail address: Jallenpeng@gmail.com

ACCEPTED MANUSCRIPT

Abstract :

This study provides new insights into the comprehensive energy and economic performances of photovoltaic shading systems (PVSS) in multi-story buildings. A numerical shading model was developed to evaluate the shading effect from an upper PVSS row on its subjacent row. Simulation models based on EnergyPlus were developed to analyze the net electricity consumption (NEC) of PVSS with different tilt angles and widths in different climates. Benefit per capacity (BC) and the cost of benefit (CB) indicators were used to analyze the economic performances of PVSS. Finally, the optimum PVSS tilt angles and widths in different cities were obtained. Harbin, Beijing, Changsha, Kunming, and Guangzhou, were selected as representative cities for different geographical and climatic conditions. The results indicate that the optimum tilt angles for PVSS installed in Harbin, Beijing, Changsha, Kunming and Guangzhou are 55°, 50°, 40°, 40° and 30°, respectively. Optimum PVSS width for all five cities is 1.156m (7 columns of standard solar cells). PVSS installed, using the optimal design scheme, in multi-story buildings have better energy-saving potentials than either rooftop photovoltaic systems or traditional power supply modes for commercial buildings in China.

Keywords: photovoltaic shading systems, numerical shading model, net electricity consumption, cost of benefit

Nomenclature

Abbreviations

AEG_{unit}	annual electricity generation per unit area
BC	benefit per capacity
CB	cost of benefit
CEB	comprehensive electricity benefit
LCC	life cycle cost
NEC	net electricity consumption
PV	photovoltaic
PVSS	photovoltaic shading systems

Symbols

H	height of each story (m)
I_m	module current at maximum power (A)
I_{sc}	short circuit current (A)
V_m	module voltage at maximum power (V)
V_{oc}	open circuit voltage (V)
α_p	profile angle (°)
α_s	solar altitude angle (°)
β	PVSS tilt angle (°)
γ	surface azimuth angle (°)
γ_s	solar azimuth angle (°)
γ_s`	pseudo solar azimuth angle (°)
δ	declination (°)
θ_z	zenith angle (°)
Φ	latitude (°)
ω	PVSS width (m)
ω_0	hour angle (°)

1. Introduction

Currently the building sector is responsible for more than one-third of all primary energy consumption and equivalent carbon emissions in developed countries [1]. Civil building energy consumption accounts for about 20% of the total energy consumption of society in China [2]. Daily operational building energy consumption, e.g. heating (space heating and hot water supply), cooling and lighting, accounts for about 80% of total building energy consumption [2]. Reducing building energy consumption would relieve the pressures of the energy crisis. Recently with the desire to use renewable energy, photovoltaic (PV) modules integration into building façades has gained wide attention and support.

Many experimental and theoretical investigations are focusing on the performance of PV modules integrated into building façades. These configurations have the potential to comprehensively improve both building energy and economic performances. Peng et al. [3-5] put forward a novel ventilated BIPV façade which lowered solar heat gain coefficient (SHGC) compared with a non-ventilated PV double-skin façade (PV-DSF). They [6] also compared the annual thermal performances of the PV façade and a normal façade. The results showed that each square meter of a south-facing normal façade replaced by a PV façade had an annual energy saving of 52.1kWh. Wang et al. [7, 8] experimentally compared the overall energy performances of a PV-DSF and a PV insulated glass unit (PV-IGU). Simulation models for the PV-DSF and PV-IGU were developed and validated against these experimental data. The results showed average energy saving potentials of 28.4% and 30% for PV-DSF and

PV-IGU, respectively. The energy performance of a semi-transparent a-Si PV-IGU was also evaluated numerically and experimentally. The results showed that compared with a single clear glass window and a Low-E glass window, the energy saving potential of the optimized PV-IGU was 25.3% and 10.7%, respectively. Koo et al. [9-11] developed a four-node-based finite element model to estimate the techno-economic performance of building-integrated PV blind (BIPB). They also explored the nonlinearity of shading effects on the techno-economic performance of BIPB and the impacts of BIPB on net-zero energy solar buildings. These findings can be used to determine the primary variables of the BIPB before implementation. Sun et al. [12,13] put forward an innovate model (combined optical, electrical and energy model) to comprehensively evaluate the performance of an office equipped with STPV (Semi-Transparent Photovoltaic) window and analyzed the effect of window design on overall energy efficiency. The results showed that the optimal design scenario of applying window integrated PV cannot only lead to a reduction in energy consumption of up to 73%, but also provide a better daylight performance compared with the conventional double glazing. Li et al. [14] combined the life cycle cost (LCC) and a pixel method for visualizing economic performance and discovered that a PV facade installation was sometimes competitive with a rooftop PV installation.

PV modules can also be used as photovoltaic shading systems (PVSS). PVSS have been widely used on low-story and multi-story buildings recently. It acts as a building power generator, which can deliver electricity at a lower cost to end users than grid electricity in certain peak-demand niche markets [15]. On the other hand, it serves as an external shading device for buildings. This will reduce the solar heat gain of exterior windows, further lowering the building cooling load in summer [16]. Several studies have examined PVSS. Sun et al. [16, 17, 18] performed a series of studies on PVSS applications in Hong Kong. System tilt angle and orientation were optimized by taking annual electricity generation and annual cooling electricity consumption as the optimal objective based on the models established in EnergyPus. Annual lighting electricity consumption, however, was not considered in their study. Yoo et al. [19, 20] held an experiment to examine the performance of a south-facing PVSS and suggested that PVSS should be used for generating electricity and providing shading for buildings. Hu et al. [21, 22] developed a series of numerical models for calculating heat transfer and electricity generation of PVSS, analyzed the net electricity consumption (NEC) of PVSS and investigated its influence on the indoor lighting environment. Zhang et al. [23] established simulation models based on EnergyPlus to explore PVSS energy-saving potential using various tilt angles and orientations in Hong Kong. The results showed that PVSS should be installed on the south-facing façade with a 20° tilt angle and could achieve greater annual overall electricity benefits than interior blinds. In fact, there are many computer simulation tools available to study renewable energy systems, such as RETScreen, HYBRID2, HOMER, TRNSYS, and EnergyPlus. From the above statements, it is seen that EnergyPlus [24] is a more comprehensive software which has been widely used to simulate and evaluate the building thermal, daylighting performance and PV power generation performance.

Despite these efforts in previous studies, optimizing PVSS comprehensive energy and economic performances in multi-story buildings has rarely been conducted. However, there are some severe issues for its application in multi-story buildings. One of the biggest issues is the shading effect from the upper PVSS row on its subjacent row. Thus, when determine and optimize the PVSS design parameters, this shading effect cannot be ignored. PVSS design parameters include its tilt angle and width. The optimum tilt angle is obviously different for various locations and climates. For example, to maximize the electricity generation of PVSS, the tilt angle should be approximate to the local latitude. However, the heating and cooling energy consumptions in different climates were also affected by the tilt angle of PVSS. In north China (i.e. heating dominated areas), to minimize the heating electricity consumption in winter, the PVSS tilt angle (the angle between the PVSS and the horizontal plane) should be larger to allow sufficiently direct sunlight into rooms. In south China (i.e. cooling dominated areas), to minimize cooling electricity consumption in summer, the tilt angle should be smaller to avoid too much heat gain from exterior windows. Therefore, in different climatic regions, there is an optimum tilt angle for PVSS installation to minimize the NEC. In addition, PVSS with various widths may result in different economic performances. Wider PVSS may generate more electricity, but its economic performance might be inferior compared with a narrower PVSS as its cost may be higher. Thus, it is necessary to analyze PVSS optimum width to obtain the best economic performance. The PVSS optimum tilt angle and width mentioned above will be affected by its shading effect. That is to say, the shading effect can change the optimum tilt angles and widths in different locations and climates. PVSSs with different widths and tilt angles result in different shading effects. This shading effect is inevitable in low latitude climates and has a significant impact on electricity generation. Electricity generated by PV modules has a nonlinear current-voltage (I-V) characteristic and there is a maximum power point (MPP) on its power-voltage (P-V) curve [25]. To maximize the electricity generation, PV modules must operate at the MPP [26-29]. Under uniform irradiance condition, PV systems have a unique Maximum Power Point (MPP) on the output characteristics curve. This MPP can be tracked by Maximum Power Point Tracking (MPPT) techniques [30, 31]. One of the major causes reducing the efficiency of PV modules is partial shading, which has a negative influence on the uniform irradiation [25]. In partial shading conditions, PV modules in an array receive different solar irradiation, therefore, there are multiple peaks on the P-V and I-V curves of the PV array. The presence of multiple peaks on the output characteristics can mislead the conventional MPPT controller to work on a local MPP, so resulting in power losses in the system [32]. In general, partial shading conditions can decrease power output and has a significant impact on the capability of delivering energy [33-36]. It was reported that ten percent (10%) shading on a conventional PV panel may cause up to an over 85% power loss and this power loss will rise as the shaded area increases [37]. Therefore, it is essential to use a special PV module configuration and analyze the shading effect on its comprehensive energy and economic performances in different cities.

This paper used a special PV module configuration that reduces the shading effect from an upper PVSS row on its subjacent row in terms of the power output. A numerical shading model was developed to analyze the PVSS shading effect and PVSS comprehensive energy performance was conducted in EnergyPlus. As the shading effect is always the same for different rows of PVSS on a multi-story building, the multi-story building model was further simplified into a two-story office building in the numerical shading model and EnergyPlus in this study. The economic performance was quantified by LCC analysis. Two optimization objectives – NEC and benefit per capacity (BC) were used to address this optimization issue. In considering shading effects, the PVSS tilt angles and widths were optimized for different cities. Finally, the optimal PVSS installation mode, which combined the tilt angles and widths for different climatic regions was obtained.

2. Methodology

This paper investigates the comprehensive energy and economic performances of PVSS in different climatic regions with taking the shading effect from the upper PVSS row on its subjacent row into account. A special PV module configuration for multi-story buildings was used to minimize the shading effect as much as possible. A numerical shading model was developed to analyze this shading effect in different cities. Simulation models based on EnergyPlus were developed to explore comprehensive PVSS energy performance, while the BC and CB were used to evaluate the PVSS economic performance.

2.1 Analytical overview

The holistic analysis workflow method appears in Figure 1. It should yield the optimal widths and tilt angles of PVSS in different climatic regions. The detailed information for each stage is as follows:

Stage I: Special PV module configuration

A special PV module configuration was used. By adopting this configuration, PV module electricity generation efficiency could be less affected by the shading effect from the upper PVSS row.

Stage II: Numerical shading model

A numerical shading model was developed. The latitude of the geographic location and PVSS width value were input, and tilt angle ranges which did not shade the subjacent row for the whole year (without considering nearby shading objects, such as buildings, trees, etc.) were obtained for each city.

Stage III: Building model in EnergyPlus

EnergyPlus was employed to analyze PVSS thermal, daylighting, and power generation performances. A multi-story office building model was established in EnergyPlus which accounts for the shading effect from the upper PVSS row on its subjacent row. The EnergyPlus PVSS power generation model was verified experimentally.

Stage IV: PVSS energy performance analysis

NEC was adopted to analyze the comprehensive energy performance and obtain the optimum PVSS tilt angles installed in various cities. PVSS NECs at various tilt angles and widths in the different regions were simulated. The optimum tilt angles for each width were obtained by maximizing the comprehensive energy performance (minimizing PVSS NECs).

Stage V: PVSS economic performance (Benefit per Capacity) analysis

BC was used to analyze the economic performance and obtain the optimum PVSS widths at the various cities. PVSS BC ($BC_{shading}$) at the optimum tilt angle for each group was calculated. The optimum PVSS widths in different cities were obtained by maximizing the economic performance (maximizing $BC_{shading}$). In addition, the BC of a traditional rooftop PV system (BC_{roof}) was calculated for comparison with the PVSS. If PVSS BC was greater than that of the rooftop PV systems, then a conclusion can be drawn that the installation of PVSS in multi-story buildings would be feasible, otherwise, it would not be feasible.

Stage VI: PVSS economic performance (Life Cycle Cost) analysis

LCC was employed to describe the detailed PVSS economic performance with the optimum widths and tilt angles. The CBs of PVSS for different climatic regions were compared with the retail electricity price for public buildings in China. If CB<0.95 RMB/kWh, then a PVSS installation in a multi-story building is feasible, otherwise, it is not feasible.

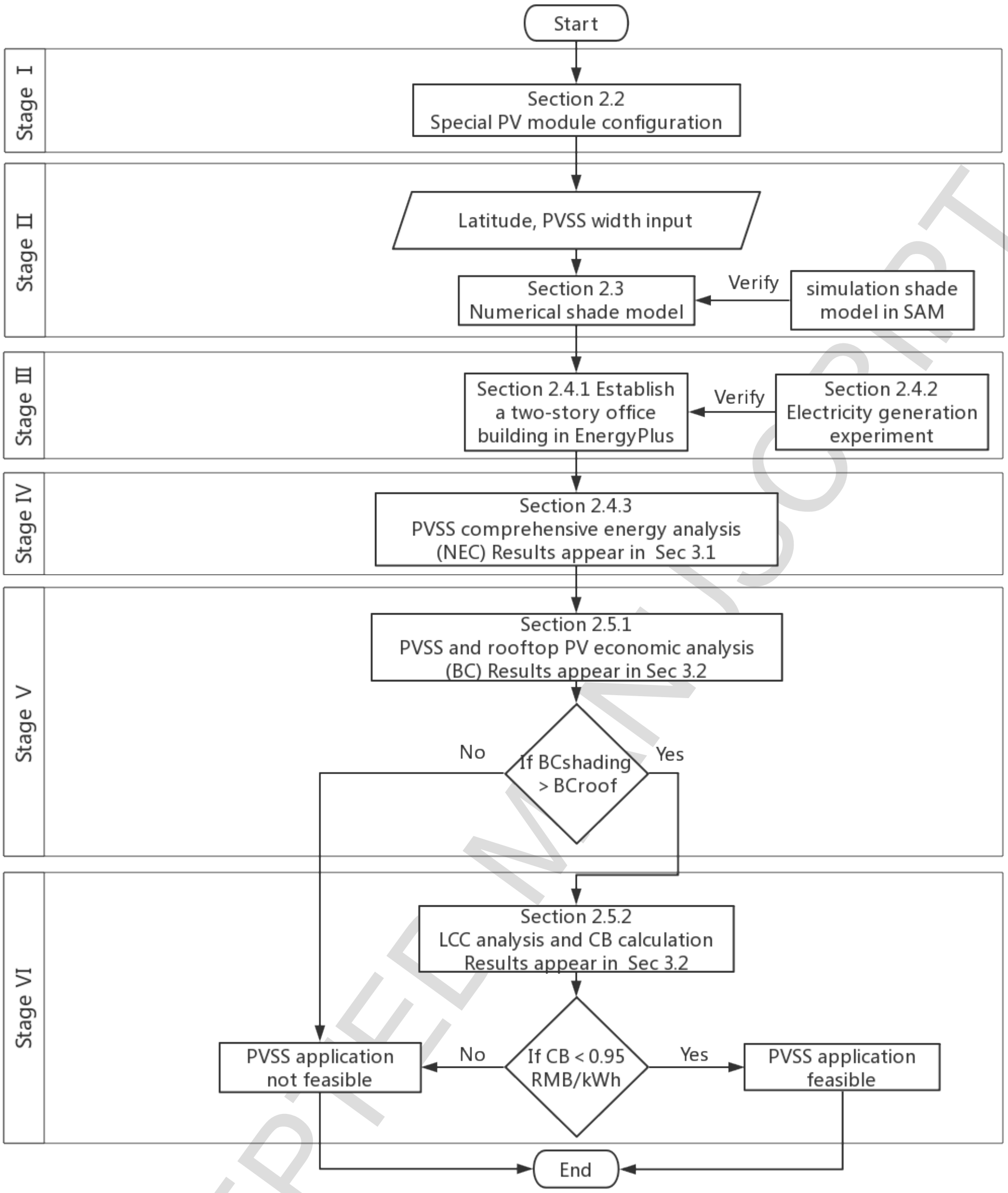

Figure 1. Flowchart of modeling and calculating optimum PVSS tilt angles and widths for different cities

2.2 Special PV model configuration

Figure 2(a) shows a traditional PV module configuration, which indicates all solar cells are connected in series. If the upper PVSS row partially shadows its subjacent row, the power generation efficiency of the subjacent row decreases significantly. Besides, it is unprocurable to simulate mismatch losses caused by partial shading in

EnergyPlus, only the power losses due to the reduction of solar radiation can be simulated. Therefore, a special PV module configuration was called for and used in this paper and appears in Figure 2(b). The solar cells are connected in a series along the length direction and in parallel across the width direction for the special PV module configuration. Compared with the traditional configuration, this special PV module configuration is insensitive to the shading effect. The upper PVSS row shading only affects the power generation of subjacent row solar cells that are shaded and it can reduce the mismatch loss to the minimum. It was reported that the maximum power increase of the special configuration is 31.93% compared with the traditional configuration [25]. Thus, the PV module with a special configuration would be less affected by upper PVSS row shading and its power generation performance can be simulated by EnergyPus.

Figure 2(a). Traditional PV module configuration for PVSS

Figure 2(b). Special PV module configuration for PVSS

2.3 PVSS Shading model

The relative geographical relation of the city to the Tropic of Cancer determines upper PVSS row shading effects on its subjacent and differs from city to city. As latitude decreases, upper PVSS row shading on its subjacent row increases. This research used an additional angle, the profile angle α_p of beam radiation on a receiver plane R that has a surface azimuth angle of γ. The profile angle is the projection of the solar altitude angle onto a vertical plane perpendicular to the plane in question, R. [38]. It is useful in analyzing the shading effect from an upper PVSS row on its subjacent row in different cities.

The solar altitude angle α_s and the profile angle α_p of the plane R are shown in Figure 3. If there is no shading at summer solstice (21 or 22 June) noon, then there will be no shading throughout the year in that location. The profile angle at summer solstice noon was used to evaluate if there exists any shading throughout the year. Going from north to south the latitudes for Harbin, Beijing, Changsha, Kunming, and Guangzhou decrease. As Guangzhou is below the Tropic of Cancer, sunlight is vertical to the horizontal surface at summer solstice noon and upper PVSS row shading on the subjacent row is inevitable. A minimum NEC can still be obtained by adjusting PVSS to the optimum tilt angle and width.

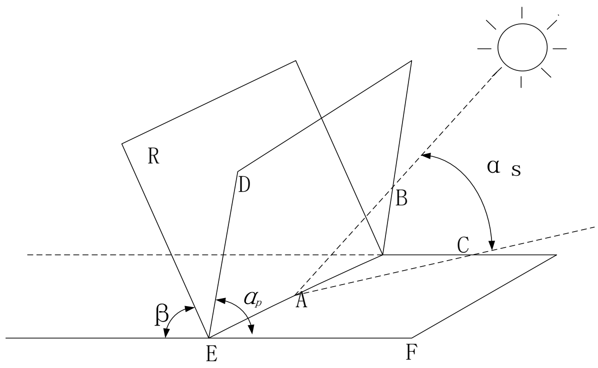

Figure 3. Solar altitude angle α_s (∠BAC) and profile angle α_p (∠DEF) for surface R

The profile angle can be calculated by the Eq. (1).

$$\tan\alpha_p = \frac{tan\alpha_s}{\cos\left(\gamma_s - \gamma\right)} \quad (1)$$

The declination δ can be found from the equation of Cooper [39] and can be calculated by Eq. (2).

$$\delta = 23.45 * \sin\frac{2\pi(284 + n)}{365} \quad (2)$$

Zenith angle (θ_z) is the angle between the vertical and the line to the sun while solar altitude angle (α_s) is the angle between the horizontal and the line to the sun, thus, zenith angle is the complement of the solar altitude angle and can be calculated by Eq. (3).

$$cos\theta_z = cos\Phi\, cos\delta\, cos\omega + sin\Phi\, sin\delta = sin\alpha_s \quad (3)$$

Solar azimuth angle (γ_s) is the angular displacement from south of the projection of beam radiation on the horizontal plane. It can be found from Braun and Mitchell [40] and calculated by Eq. (4) - (10).

$$\gamma_s = C_1 C_2 \gamma_s^{`} + C_3\left(\frac{1 - C_1 C_2}{2}\right)180 \quad (4)$$

where $$\sin\gamma_s^{`} = \frac{sin\omega_0 sin\delta}{sin\theta_z} \quad (5)$$

or $$\tan\gamma_s^{`} = \frac{sin\omega_0}{sin\Phi\, cos\omega_0 - cos\Phi\, tan\delta} \quad (6)$$

$$C_1 = \begin{cases} 1 \text{ if } |\omega_0| < \omega_{ew} \\ -1 \text{ otherwise} \end{cases} \quad (7)$$

$$C_2 = \begin{cases} 1 \ \ if\ \phi(\phi - \delta) \geq 0 \\ -1 \quad \text{otherwise} \end{cases} \quad (8)$$

$$C_3 = \begin{cases} 1 \quad \omega_0 \geq 0 \\ -1 \text{ otherwise} \end{cases} \quad (9)$$

$$\cos\omega_{ew} = \frac{tan\delta}{tan_{\emptyset}} \quad (10)$$

Surface azimuth angle (γ) is the deviation of the projection on a horizontal plane of the normal to the surface from the local meridian. With zero due south, east negative and west positive. In this research, all PVSS surfaces face south and the surface azimuth angle is zero.

The cross-section view of a PVSS installed in multi-story buildings appears in Figure 4. The relationship between H, β, ω, and α_p are calculated in Eqs. (11). The tilt angle β is the angle between the PVSS and the horizontal plane. The lower ends of the PVSS and the head of windows are kept at the same height.

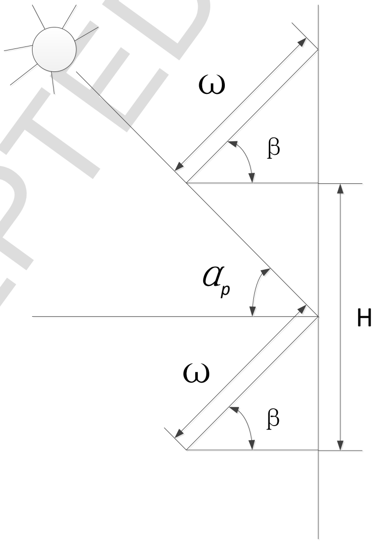

Figure 4. Cross-section of PVSS on a multi-story building

$$\mathrm{H} = \omega \sin\beta + \omega \cos\beta \tan\alpha_p \leq 3.9m \quad (11)$$

The detailed information about the dimensions of the office building and PVSS are obtained from a simulation model established in EnergyPlus (Sec. 2.4.1). Story height

(H) is 3.9m. The PVSS consists of 9 PV modules and the PV module includes many solar cells (156mm*156mm) that are separated by 8mm solar cell gaps. The number of cells along the length direction is 10 while the number of cells along the width direction ranges from 4 to 7. PV module length is 1.65m, but width varies from 0.664m to 1.156m corresponding to the 4-7 solar cells in parallel. The tilt angle (β) ranges, for which no shading would occur in the five cities, can be calculated through Eqs. (1) to (11). The results appear in Table 1. Due to the low solar altitude angle, there is no shading effect from the upper PVSS row on its subjacent row in Harbin regardless of tilt angles or widths. Partial shading occurs in Beijing when the PVSS tilt angle ranges from 7° to 27° with a width of 1.156m. It has no effect on the analysis of the optimum tilt angle because the optimum tilt angle for Beijing is outside this range. Therefore, shading effects for Harbin and Beijing need not be analyzed. The shading from the upper PVSS row has a significant impact on the performance of the subjacent row in Changsha, Kunming, and Guangzhou. This is especially true for Guangzhou where the shading effect is inevitable around the summer solstice due to its proximity to the Tropic of Cancer. Therefore, PVSS shading effect on its comprehensive energy and economic performances in these three cities warrants closer investigation.

Table 1. PVSS tilt angle ranges without shading for various widths

City	Latitude (°)	Width (m)	Tilt range for no shading
Harbin	45.75	0.664	[0°,90°]
		0.828	[0°,90°]
		0.992	[0°,90°]
		1.156	[0°,90°]

Beijing	39.8	0.664	[0°,90°]
		0.828	[0°,90°]
		0.992	[0°,90°]
		1.156	[0°,7°]∪[27°,90°]
Changsha	28.22	0.664	[65°,90°]
		0.828	[71°,90°]
		0.992	[75°,90°]
		1.156	[78°,90°]
Kunming	25.02	0.664	[81°,90°]
		0.828	[83°,90°]
		0.992	[85°,90°]
		1.156	[86°,90°]
Guangzhou	23.17	0.664	Ø
		0.828	Ø
		0.992	Ø
		1.156	Ø

A shading loss simulation model was established by 3D shading calculator in System Advisor Model (SAM) [41] to verify the accuracy of the numerical shading model. The SAM 3D shading calculator uses a sun position algorithm and a three-dimensional drawing of a photovoltaic array to generate hour-by-month tables of shading loss percentages. The shading effect from the upper PVSS row on its subjacent row can be approximately quantified by shading loss. Shading loss at certain times is the ratio of the shaded area to the total active area and is calculated in SAM. The shading losses of PVSS with different widths and tilt angles at summer solstice noon were simulated in SAM for Changsha and Kunming. It ranges from 0%-100%, and 0% represents no shading while 100% is full shading. Figure 5 shows the PVSS shading losses on the summer solstice at noon in Changsha. For each width, the shading losses of PVSS decline continuously as the tilt angle increases. The simulation results are similar to the calculation results in Table 1. The simulation results for Kunming in Figures 6 also nearly fit with the calculated results in Table 1.

As Guangzhou crosses through the Tropic of Cancer, the sunlight is perpendicular to the ground on the summer solstice at noon, which lead to a 100% shading loss for PVSS with all widths and tilt angles. Compared with the numerical shading model, there are some assumptions about the shading loss in SAM, for example, the sun position is at the midpoint of each hour on the 14th day of each month. Therefore, the numerical shading model developed here is more accurate to analyze the shading effect from the upper PVSS row on its subjacent row and facilitates the analysis of PVSS shading effect on its comprehensive energy and economic performances in different cities.

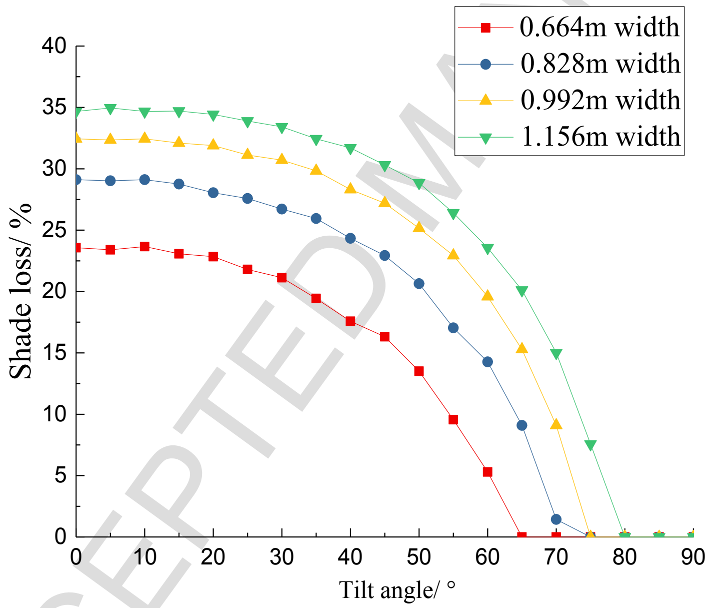

Figure 5. PVSS shading loss at summer solstice noon in Changsha

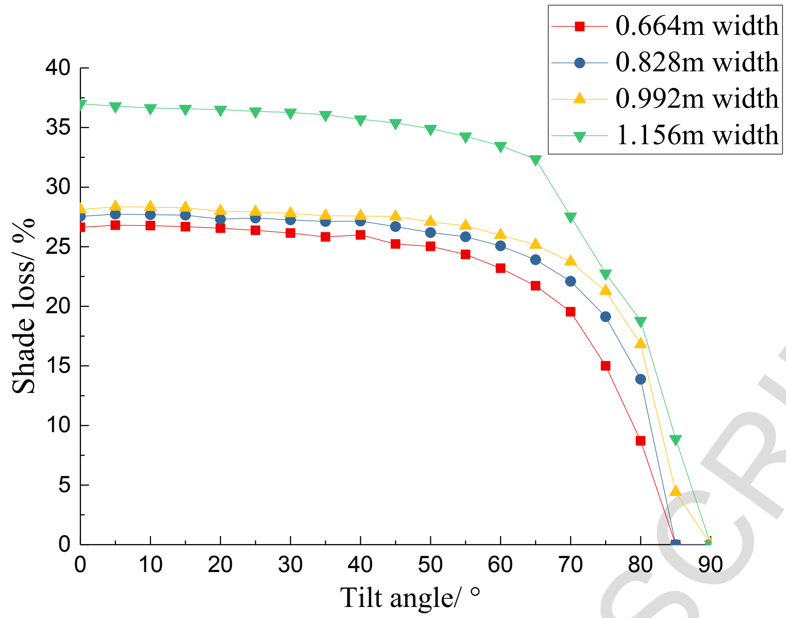

Figure 6. PVSS shading loss at summer solstice noon in Kunming

2.4 Simulation and analysis of comprehensive PVSS energy performance

A set of simulation models were developed in EnergyPlus to analyze the comprehensive PVSS energy performances in different cities around China. The PVSS electricity generation model was validated against the experimental data. In addition, NEC was defined to quantify the PVSS comprehensive energy performance and the optimum tilt angles of each width were obtained by minimizing the NECs.

2.4.1 EnergyPlus simulation model

The simulation model established in EnergyPlus was based on a typical Chinese multi-story office building. Building model dimensions are 16m (length) * 8m (width) * 3.9m (story height). The distance from the roof to the upper edge of the window is 0.84m. The distance from the floor to the lower edge of the window is 1.5m. According to building energy efficiency standards in China [42], there are different requirements for thermal properties of building envelopes in different climates. In this research, all U values of external walls, roofs, floors and windows in five climates were set to satisfy the thermal requirements. Double clear glazing system (U-value 2.78W/m^{2}k) were used for window systems. Besides, each floor has 9 PV modules installed on its south-facing façade and constitute a PVSS (Fig. 8). Two PVSSs were set in the model to analyze the shading effect on comprehensive energy and economic performances. The PV modules in the upper PVSS row are defined as PV_{21}, PV_{22}, PV_{23}, PV_{24}, PV_{25}, PV_{26}, PV_{27}, PV_{28}, PV_{29} and in the subjacent PVSS row are defined as PV_{11}, PV_{12}, PV_{13}, PV_{14}, PV_{15}, PV_{16}, PV_{17}, PV_{18}, PV_{19}. The PVSS tilt angle ranges from 0° to 90°, at 5° interval. Key parameters of the PV module with 60 solar cells modelled in EnergyPlus are shown in Table 2. The widths of the PV module are set as 0.664m, 0.828m, 0.992m, 1.156m, as presented in Table 3. The current at the maximum power point of the PV module with various widths can be calculated by Eq. (12). The short circuit current is proportional to the number of solar cells in parallel. Open circuit voltage and the voltage at the maximum power point were simplified as constants. Shunt resistances of PV modules with various widths can be calculated by EES software.

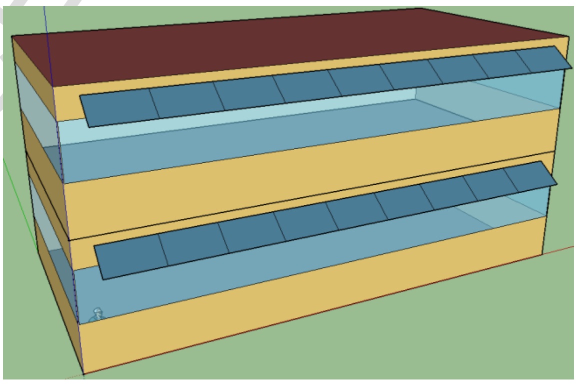

Figure 7. The EnergyPlus simulation model

$$\mathrm{FF} = \frac{I_m V_m}{I_{sc} V_{oc}} \tag{12}$$

Table 2. PV module key parameters

Parameters	Values
Solar cell type	Poly-Si
Solar cell size (mm*mm)	156*156
Solar cell gap (mm)	8
Number of cells in width	6
PV panel width (m)	0.992
PV panel area (m^2)	1.637
Transmittance absorptance product	0.9
Semiconductor bandgap (eV)	1.12
Short circuit current (A)	54
Open circuit voltage (V)	6.4
Module current at maximum power (A)	51
Module voltage at maximum power (V)	5.1
Shunt resistance (Ω)	776
Reference temperature (℃)	25
Reference insolation (W/m^2)	1000
Temperature coefficient of short circuit current(A/K)	0.00477
Temperature coefficient of open circuit voltage(V/K)	-0.1222
Module heat loss coefficient (W/m^2*K)	30
Total heat capacity (J/m^2*K)	50000

Table 3. PV module parameters at various widths

Main parameters	Values	Values	Values	Values
Solar cell type	Poly-Si	Poly-Si	Poly-Si	Poly-Si
Solar cell size (mm*mm)	156*156	156*156	156*156	156*156
Solar cell gap (mm)	8	8	8	8
Number of cells in width	4	5	6	7
PV panel width (m)	0.664	0.828	0.992	1.156
PV panel area (m^2)	1.096	1.366	1.637	1.907
Short circuit current (A)	36	45	54	63
Open circuit voltage (V)	6.4	6.4	6.4	6.4
Module current at maximum power (A)	34	42.5	51	59.5
Module voltage at maximum power (V)	5.1	5.1	5.1	5.1
Shunt resistance (Ω)	1000	1000	776	630

The heat transfer model, daylighting model and PV power generation model in EnergyPlus were used to analyze PVSS thermal, daylighting and power generation performances. The weather data of Solar and Wind Energy Resource Assessment

(SWERA) were adopted for the simulation.

The heat transfer model was employed to simulate the hourly heating and cooling load. In Changsha, Kunming, and Guangzhou, an air source heat pump was used to provide cooling in summer and heating in winter. The COP for cooling was 3.0 and 2.75 for heating. In Harbin and Beijing, a natural gas-fired boiler was used for heating and its efficiency was 0.8. Air source air conditioning was used to provide cooling in summer and its COP was set to be 3.0. The natural gas energy used by the boiler was converted into electrical energy using a conversion factor to analyze NEC.

The daylighting model was used to determine the daylight illuminance at reference points. As the PVSS reduces the available daylight getting into the office, electricity consumption to provide artificial lighting is expected to increase. When the illuminance level in a zone is lower than the design value, artificial lighting will be turned on to compensate. The daylighting model was used to simulate artificial lighting electricity consumption. The lighting control points were set in the middle of each area at a height of 0.75 m. The illumination level and lighting density were set to be 300 lux and 9W/m^2, respectively.

The PV power generation model was used to simulate the PVSS electricity generation. There are three different power generation models in EnergyPlus and Equivalent One-Diode model was adopted in this paper because it is relatively accurate for predicting the polycrystalline silicon solar cells' performance [43].

2.4.2 Model verification

A test rig was built to verify the accuracy of the PVSS power generation model. The building dimensions are 4 (length) × 4 (width) × 2.5 (height). The size of the PV module is 1.65m (length) * 0.992m (width) and the PV cell type is polycrystalline silicon. The PV module's rated power is 260 W and the efficiency is 15.9%. The measurement period was from September 2014 to April 2015. Main equipment adopted in this experiment includes an inverter, MPPT charge controller, I-V curve tracer, pyranometers, data loggers etc. A massive amount of data, such as the power and energy output, the I-V curves, the solar radiation and temperature, has been collected and recorded. Figure 8 compares the generic PVSS model in EnergyPlus (left) and the real test rig (right).

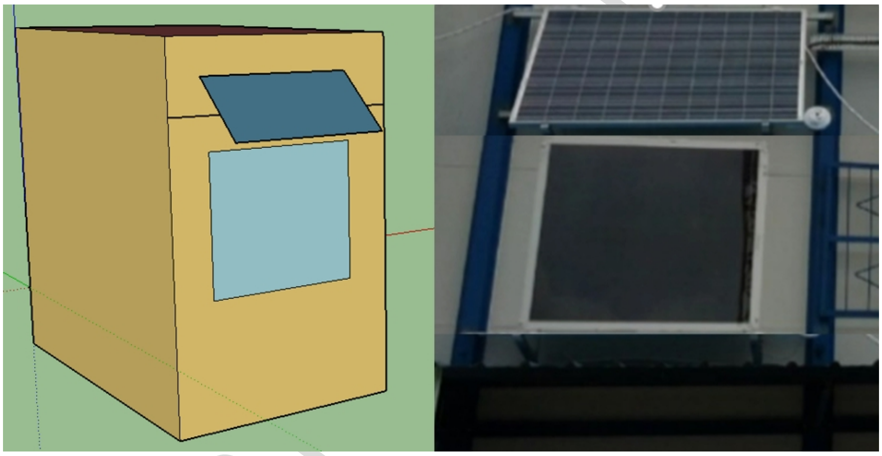

Figure 8. Generic PVSS model in EnergyPlus (left) and real test rig (right)

From the measurement results in January 2015, the daily mean ambient temperature ranges from 13.3°C to 21.4°C, the lowest value occurs on Jan 13th, and the highest value occurs on Jan 6th. The daily solar irradiation incident on PV module (7am to 5pm) on Jan 5th, 7th, 12th, 13th, 29th and 31st are relatively low because of the overcast weather condition (around 200Wh), while it is relatively high on sunny days, such as Jan 6th, 19th, 22th and 23th (around 5000Wh). Figure 9 compares the measured electricity generation and the simulated electricity generation in January

2015. The dates with lower solar irradiation lead to lower power generation, and vice versa, which indicates that the dominant factor contributing to the power generating is solar irradiation. Besides, the daily simulated electricity generation agrees well with the daily measured electricity generation. In terms of the monthly electricity generation, the measured electricity generation in January 2015 was 22.6 kWh. The corresponding simulation figure was 23.5 kWh. The deviation was 3.8%. Therefore, the simulation model can accurately simulate the PVSS electricity generation in other climatic regions.

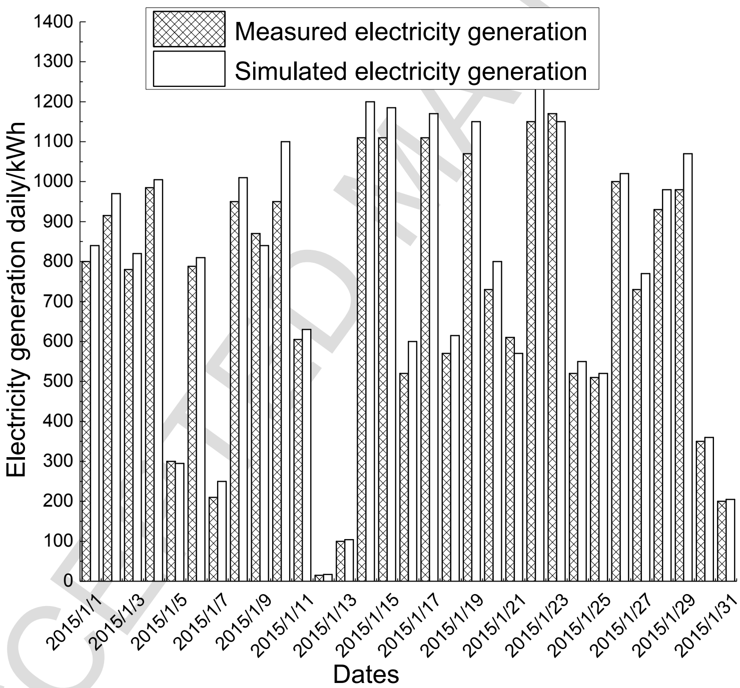

Figure 9. Comparison between experimental and simulation results

2.4.3 Comprehensive PVSS energy performance indicators

Net electricity consumption (Q_{nec}) consists of heating and cooling energy consumption, lighting electricity consumption and PVSS electricity generation, as shown in Eq. (13). The PVSS optimum tilt angles installed in the different cities can be determined by minimizing NEC.

$$Q_{nec} = Q_a + Q_l - Q_e \tag{13}$$

Q_{nec} is the net electricity consumption of the building with PVSS. Q_a is the annual heating and cooling energy consumption. Q_l is the annual lighting electricity consumption. Q_e is the annual PVSS electricity generation.

2.5 Analysis of PVSS economic performance

$BC_{shading}$ was defined to quantify PVSS economic performance, and the optimum PVSS widths in five cities can be determined by maximizing $BC_{shading}$. Economic performance comparison between PVSS and a traditional rooftop PV system were conducted to determine if the PVSS was economically feasible. Finally, an LCC tool was employed to explore the detailed economic benefits of PVSS with optimum widths and tilt angles in different climatic regions.

2.5.1 PVSS economic performance indicator

Comprehensive electricity benefit (Q_{ceb}) was employed to evaluate the PVSS economic performance. $BC_{shading}$ represents the comprehensive electricity benefit of per unit installed PVSS capacity, as described by Eq. (14) and Eq. (15).

$$Q_{ceb} = Q_e + (Q_{a0} - Q_a) + (Q_{l0} - Q_l) \tag{14}$$

$$BC_{shading} = \frac{Q_{ceb}}{Q_{cap}} \tag{15}$$

Q_{ceb} is the PVSS comprehensive electricity benefit. $BC_{shading}$ is the comprehensive electricity benefit of per unit installed PVSS capacity. Q_a is the annual heating and cooling energy consumption of the PVSS building. Q_{a0} is the annual heating and cooling energy consumption of the non-PVSS building. Q_l is the annual lighting electricity consumption of the PVSS building. Q_{l0} is the annual lighting electricity consumption of the non-PVSS building. Q_e is the annual PVSS electricity generation. Q_{cap} is the installed PVSS capacity.

Compared with the PVSS, a normal rooftop PV system has advantages in electricity generation, but it has a limited effect on reducing the building energy consumption. To compare the economic performance between a PVSS and a normal rooftop PV system, the optimum tilt angles for maximizing the electricity generation (Q_e) of a rooftop PV system were simulated in EnergyPlus and the electricity generation of a rooftop PV system with its optimum tilt angles (50°, 45°, 35°, 35°, 35° for Harbin, Beijing, Changsha, Kunming and Guangzhou, respectively) and the same optimum widths as PVSS were obtained from the calculated results. The benefit per capacity of a rooftop PV system (BC_{roof}) was calculated by Eq. (16).

$$BC_{roof} = \frac{Q_e}{Q_{cap}} \tag{16}$$

BC_{roof} is the electricity benefit of per unit installed capacity of a rooftop PV system. Q_e is the annual rooftop PV system electricity generation. Q_{cap} is the installed rooftop PV system capacity.

2.5.2 PVSS LCC analysis

The life cycle cost of a PV system consists of total fixed and operating costs over its life expressed in present value [44-48]. The major cost of a PV system includes acquisition cost, operating and maintenance costs [49]. In this study, the total life-cycle cost of a PVSS is the sum of present worth (PW) of PV modules, inverter, installation, operation and maintenance cost, and financial cost [50-52]. The main assumptions for LCC boundary and parameter estimation are in Table 4.

Table 4. Main assumptions for LCC analysis [53]

Classification	Detailed description
Analysis period	25 years
Analysis method	Present worth method
Real discount rate (i)	5%
PV system price	5.2RMB/W
K_i	20%
K_m	2%
K_l	15%
i_l	7%
a	0.95RMB/kWh

In this paper, all past and future capital investments were summed to present value and LCC can be calculated by Eq. (17),

$$\mathrm{LCC} = P_l + P_i + P_{mo} + P_f \tag{17}$$

P_l is the initial investment cost for a PV system including PV modules and inverters. P_i is the installation cost. P_{mo} is the maintenance and operation cost. P_f is the financial cost.

Installation costs (P_i), annual maintenance and operation costs (P_{amo}) are each estimated in accordance with a certain proportion of the total initial investment cost. It can be calculated by Eq. (18) and (19),

$$P_i = P_l \times K_i \tag{18}$$

$$\mathrm{P}_{amo} = P_l \times K_{mo} \tag{19}$$

The annual financial expense (P_{af}) is related to the loan amount and lending rate, as shown in Eq. (20),

$$\mathrm{P}_{af} = P_l \times K_l \times i_l \tag{20}$$

Total maintenance, operation costs (P_{mo}) and financial expenses (P_f) during n year period are defined as Eq. (21) and (22),

$$P_{mo} = P_{amo}\frac{[(1+i)^n - 1]}{i(1+i)^n} \tag{21}$$

$$P_f = P_{af}\frac{[(1+i)^n - 1]}{i(1+i)^n} \tag{22}$$

The total LCC is annualized by using a capital recovery factor (CRF) taken from Raman and Tiwari [54]. It can be calculated by Eq. (23),

$$\mathrm{CRF} = i[\frac{(1+i)^n}{(1+i)^n - 1}] \tag{23}$$

The annualized total cost (C_a) is a measure to represent the amount of capital required per year to use the system. It is defined as Eq. (24),

$$C_a = CRF \times LCC \tag{24}$$

PVSS CB can be calculated from dividing the annualized total cost by the comprehensive electricity benefit per year, as shown in Eq. (25),

$$\mathrm{CB} = \frac{C_a}{Q_{ceb}} \tag{25}$$

As for above LCC calculation method, the cost accuracy relies on the quality of data and the data uncertainty is a well-recognized issue [55-57], especially for results that heavily relied on the future tendency of economic data. There are some uncertainties resulting from assumptions during the LCC analysis. For example, the assumption of constant discount rate ignores the possibility of variations over the life cycle of the PV system. In fact, the discount rate might change as the changes of national monetary and fiscal policies. Another assumption is the energy price, which also leads to uncertainty. Besides, the estimation of PV module price and the maintenance cost also result in uncertainties. The last uncertainty for LCC forecasting is to determine the system service life [58]. Even though there are numerous handbooks, manuals and guidelines published on life-cycle cost analysis and LCC software applications are becoming more and more prevalent as time progresses, the comprehensive LCC uncertainty analysis is still a severe issue. Uncertainty analysis as well as some tough problems, such as political relevance, ethical concerns, attitude towards risk, etc., still need to be explored in further study.

3 Results and discussions

This section analyzes PVSS comprehensive energy and economic performances. First, the annual NECs of PVSS with different widths and tilt angles were compared to obtain the optimum tilt angles for the various cities. Monthly NEC of PVSS with 1.156m width and its optimum tilt angle was also analyzed to explore the PVSS seasonal effect on buildings' energy performance. A sensitivity analysis was conducted on tilt angle and width to investigate the dominant factor influencing the NEC. Then, the BCs of PVSS with optimum tilt angles at each width were analyzed to determine the optimum widths. Finally, the CBs of PVSS with optimum tilt angles and widths in various climatic regions were compared with public buildings' retail electricity prices to determine whether PVSS is economically feasible to be applied in a certain climatic region.

3.1 Comprehensive PVSS energy performance

Different locations have different shading effects. The five cities were grouped into two region types. Group One is Harbin and Beijing. Group Two is Changsha, Kunming, and Guangzhou. There is no shading effect from the upper PVSS row on its subjacent row in Group One. In Group Two, upper PVSS row shading effect is inevitable. The comprehensive energy performances for the five climatic cities were studied using a two-story office building model in EnergyPlus.

3.1.1 Group one: shading effect free cities

Figures 10 and 11 illustrate PVSS AEG_{unit} (annual electricity generation per unit area) and NEC at various tilt angles and widths in Harbin and Beijing, respectively. For all widths, AEG_{unit} initially increases and then decreases as the tilt angle increases. The maximum AEG_{unit} generated by a PVSS in Harbin is 267.23kWh/m^2 with a 50° tilt angle and 1.156m width, which is more than twice the minimum AEG_{unit} generated by a PVSS with a 0° tilt angle and 0.664m width. The maximum AEG_{unit} generated by a PVSS in Beijing is 266.83kWh/m^2 with a 45° tilt angle and 1.156m width, which is also more than twice the minimum AEG_{unit} generated by a PVSS with a 0° tilt angle and 0.664m width. In contrast, NEC initially decreases and then increases as tilt angle increases. The optimum tilt angles are 45°, 50°, 50° and 55° respectively corresponding to the width increasing from 0.664 m to 1.156 m in Harbin and the corresponding data are 40°, 45°, 45°, and 50° respectively in Beijing. As PVSS width increases, tilt angle needs to increase to let in more daylight, in order to reduce artificial lighting electricity consumption. Therefore, the optimum tilt angle will increase as width increases. The minimum PVSS NEC in Harbin was 3098.7kWh corresponding to a 55° tilt angle and 1.156m width. This is slightly more than a half of the maximum NEC generated by a PVSS with a 0° tilt angle and 0.664m width. In Beijing, the minimum NEC of a PVSS is 756.24kWh corresponding to a 50° tilt angle and 1.156m width, which is significantly less than the maximum NEC of a PVSS with a 90° tilt angle and 0.664m width.

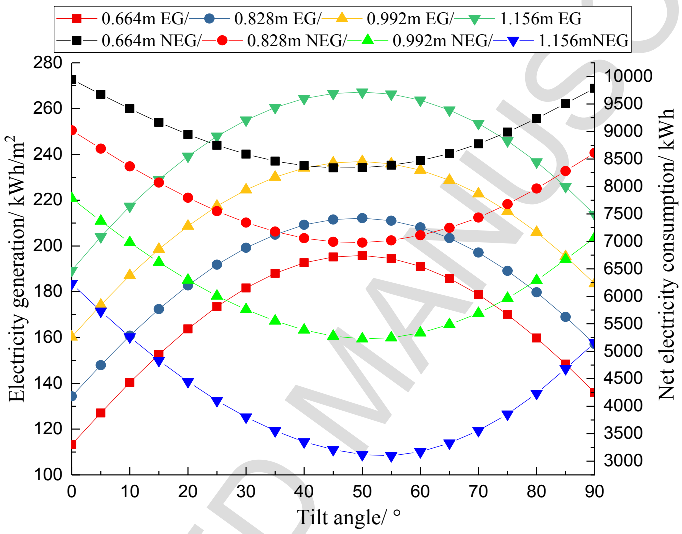

Figure 10. PVSS AEG_{unit} and NEC at various widths in Harbin

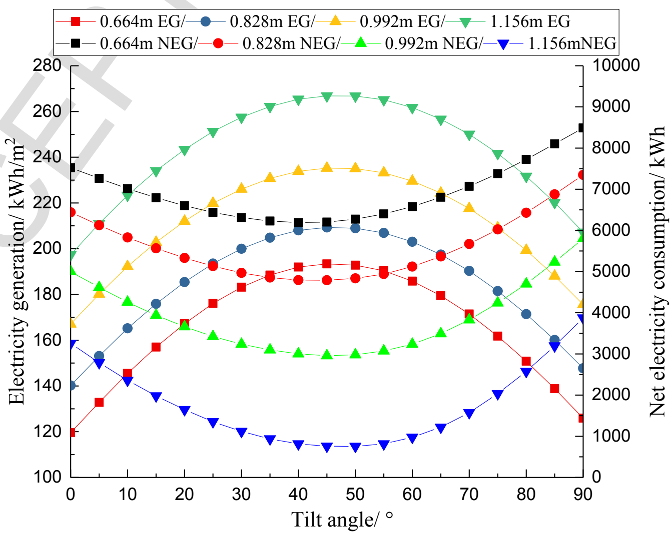

Figure 11. PVSS AEG_{unit} and NEC at various widths in Beijing

3.1.2 Group two: cities with shading effects

Figures 12-14 illustrate PVSS AEG_{unit} and NEC at various widths and tilt angles in Changsha, Kunming, and Guangzhou, respectively. For each width, the AEG_{unit} initially increases and then decreases as tilt angle increases. The maximum PVSS AEG_{unit} in Changsha is 187.72kWh/m^2 with a 40° tilt angle and 1.156m width, which is three times the minimum AEG_{unit} of a PVSS with a 90° tilt angle and 0.664m width. The maximum AEG_{unit} of a PVSS in Kunming is 238.42 kWh/m^2 with a 40° tilt angle and 1.156m width, which is nearly three times as much as the minimum PVSS AEG_{unit} with a 90° tilt angle and 0.664m width. The maximum PVSS AEG_{unit} in Guangzhou is 199.70kWh/m^2 with a 40° tilt angle and 1.156m width, which is also nearly three times as much as the minimum PVSS AEG_{unit} with a 90° tilt angle and 0.664m width. It is also seen that the optimum tilt angles for maximizing the AEG_{unit} of PVSS are larger than that of a rooftop PV system. This is because a larger PVSS tilt angle will contribute to a smaller shading effect, such that increasing its electricity generation. On the contrary, the NEC initially decreases and then increases as tilt angle increases. PVSS optimum tilt angles in Changsha are 35°, 40°, 40°, and 40° respectively corresponding to width increasing from 0.664 m to 1.156 m. The corresponding data for Kunming is 35°, 35°, 35°, and 40°, respectively. For Guangzhou they are 25°, 30°, 30°, and 30°, respectively. Furthermore, the minimum NEC generated by a PVSS in Changsha is 5772.86kWh, which is only half of the maximum NEC of the PVSS with a 90° tilt angle and 0.664m width. The minimum NEC generated by a PVSS in Kunming is -1324.48kWh (the heating and cooling electricity consumption is 6154.01kWh, the lighting electricity consumption is 700.61kWh and the electricity generation of PVSS is 8179.10kWh). This is far less than the maximum NEC generated by the PVSS with a 90° tilt angle and 0.664m width. The minimum NEC of the PVSS in Guangzhou is 9420.49kWh, which accounts for about 40% of the maximum NEC of the PVSS with a 90° tilt angle and 0.664m width.

As has been mentioned, NEC is determined by heating energy consumption in winter, cooling energy consumption in summer, lighting electricity consumption and PVSS electricity generation of the whole year. In this paper, to obtain the optimum fixed annual tilt angle for each width, we investigated the PVSS annual energy performance. Nevertheless, monthly NEC analysis could reflect the PVSS seasonal energy performance. Figure 15 shows the monthly electricity consumption and NEC for the PVSS with 1.156m width and the optimum tilt angle (40°) in Changsha. The minimum electricity generation occurs in winter while the maximum one occurs in summer. However, the NECs in spring and autumn are greater than that in summer and winter. This is mainly because the cooling energy consumption in summer and the heating energy consumption in winter accounts for a large percentage of the total energy consumption in Changsha. The NECs are negative in Mar., Apr., Oct. and Nov., which indicates that the PVSS electricity generation could meet the building electricity demand during this period.

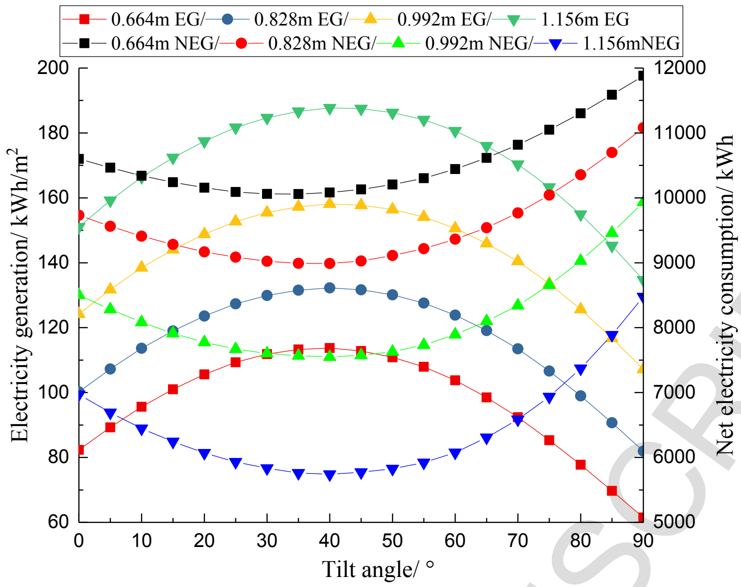

Figure 12. PVSS AEG_{unit} and NEC at various widths in Changsha

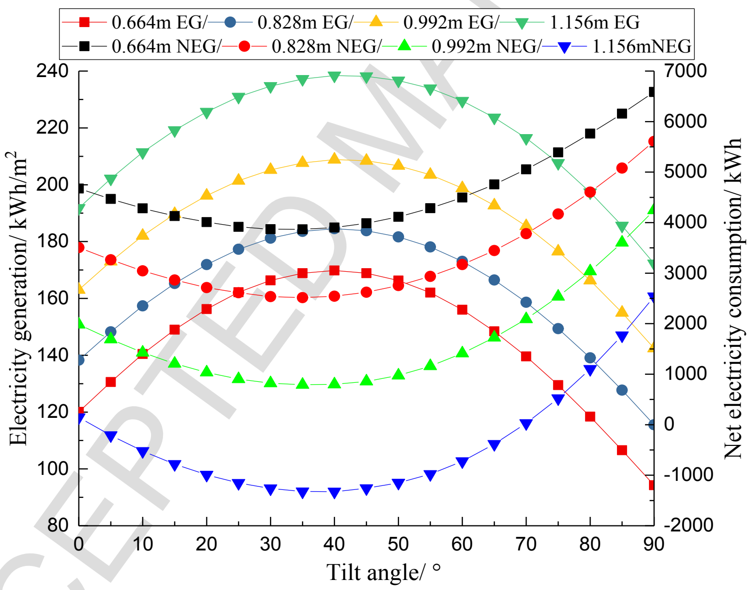

Figure 13. PVSS AEG_{unit} and NEC at various widths in Kunming

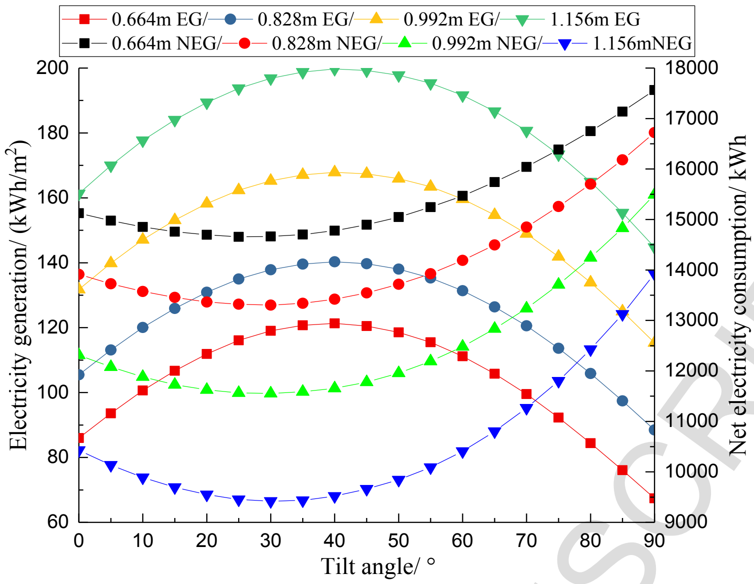

Figure 14. PVSS AEG_{unit} and NEC at various widths in Guangzhou

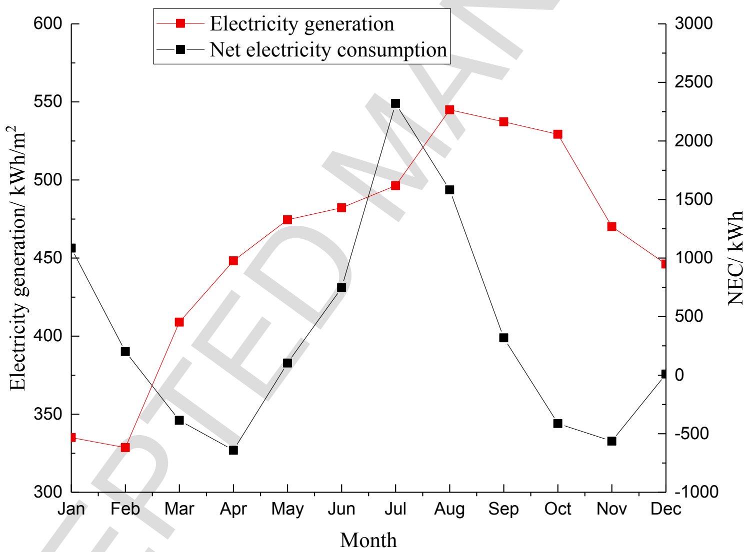

Figure 15. PVSS monthly electricity generation and NEC at 40° tilt angle and 1.156m width in Changsha

3.1.3 NEC sensitivity analysis

Building NEC is mainly affected by PVSS tilt angle and width in this study. Thus, a sensitivity analysis was conducted for these two factors. The PVSS tilt angle varies from 0° to 90° with an interval of 5° while the total width varies from 4 to 7 times of the width (0.664m) of a single solar cell's width. Figure 10 through 14 show that the PVSS width has a greater impact on the building NEC than the tilt angle. In other word, the building NEC is more sensitive to the PVSS width. Taking Harbin as an example, the building NEC has an average variation of 245.76kWh whenever the tilt angle changes 5° while it has an average variation of 1750kWh as the width changes per 0.164 m. Thus, it is necessary to optimize the PVSS width for improving buildings' energy performance.

3.2 PVSS economic performance

The PVSS width, on the one hand, has a sensitive impact on buildings' energy performance. On the other hand, determines its economic performances to some extent. Therefore, it is necessary to analyze PVSS BC, which was used to obtain the optimum widths. BC results appear in Table 5. When PVSS widths are all 1.156m in the five climatic regions, BC reaches its maximum values. The corresponding values for five cities (Harbin, Beijing, Changsha, Kunming, and Guangzhou) are 1.72, 1.87, 1.35, 1.79 and 1.74kWh/W, respectively. Therefore, the optimum widths of PVSS in the five climatic regions are all 1.156m while the corresponding optimum tilt angles are 55˚, 50˚, 40˚, 40˚, and 30˚. Besides, the maximum BC occurs in Beijing while the minimum one belongs to Changsha. This is because the solar radiation in Beijing is strong and the power generation is relatively higher; A larger optimum tilt angle also contribute to the electricity generation growth; And the larger optimum tilt angle has a less impact on reducing the indoor illuminance, which will contribute to reducing the lighting electricity consumption; Even though the existence of PVSS will significantly increase the heating electricity consumption in winter, it can reduce the cooling electricity consumption in a large proportion in summer. This is the opposite effect in Changsha. Solar radiation in Changsha is relatively weak and the power generation is relatively lower; The smaller optimum tilt angle also has a negative impact on electricity generation; And the smaller optimum tilt angle has a dramatic impact on reducing the indoor illuminance, which will result in increasing the lighting electricity consumption; The PVSS existence has almost the same effect on the cooling electricity consumption reduction in summer and heating electricity consumption increase in winter. From Table 6, the BCs of rooftop PV systems in the five cities (Harbin, Beijing, Changsha, Kunming, and Guangzhou) were calculated as 1.28, 1.47, 0.97, 1.23, and 1.05kWh/W, respectively, Thus, compared with rooftop PV systems, PVSS have the better economic performances.

Table 5. PVSS CEB and BC at different widths and optimum tilt angles.

City	PVSS width (m)	Optimum tilt angle (°)	CEB (kWh)	PVSS BC (kWh/W)
Harbin	0.664	45	4139.86	1.33
	0.828	50	5499.78	1.41
	0.992	50	7201.14	1.54
	1.156	55	9378.81	1.72
Beijing	0.664	40	4793.01	1.54
	0.828	45	6194.98	1.59
	0.992	45	8026.51	1.71
	1.156	50	10228.67	1.87
Changsha	0.664	35	3041.82	0.97
	0.828	40	4112.24	1.05
	0.992	40	5551.46	1.19
	1.156	40	7359.7	1.35
Kunming	0.664	35	4594.98	1.47
	0.828	35	5947.31	1.52
	0.992	35	7673.01	1.64
	1.156	40	9787.41	1.79

Guangzhou	0.664	25	4259.85	1.36
	0.828	30	5612.32	1.44
	0.992	30	7363.03	1.57
	1.156	30	9496.5	1.74

Table 6. BC of rooftop PV systems in different cities

City	Harbin	Beijing	Changsha	Kunming	Guangzhou
BC of rooftop PV systems	1.28	1.47	0.97	1.23	1.05

Table 7 provides detailed PVSS economic performances at optimum tilt angles and optimum widths for five cities. PVSS CBs in all five cities is less than 0.95 RMB/kWh (the retail electricity price for Chinese public buildings), which indicates that the PVSS would have better economic performances in all cities. This is particularly true for Beijing and Kunming, where the CB is 0.452 and 0.472 RMB/kWh and is far below the retail electricity price for local public buildings. Therefore, PVSS is applicable in these five climatic cities.

Table 7. PVSS CB at optimum tilt angles and optimum widths

City	Optimum width/m	Optimum tilt angle/°	CEB/ kWh	Total cost of PV system/ RMB	Cost of installation/ RMB	Total financial expense/RMB	Total cost of maintenance and operating /RMB	CB/ (RMB/kWh)
Harbin	1.156	55	9378.81	28402.92	5680.58	2707.05	5156.29	0.493
Beijing	1.156	50	10228.67	28402.92	5680.58	2707.05	5156.29	0.452
Changsha	1.156	40	7359.7	28402.92	5680.58	2707.05	5156.29	0.628
Kunming	1.156	40	9787.41	28402.92	5680.58	2707.05	5156.29	0.472
Guangzhou	1.156	30	9496.5	28402.92	5680.58	2707.05	5156.29	0.487

4 Conclusions

This study investigated the comprehensive energy and economic performances of PVSS installed in multi-story buildings in different climatic regions. Due to upper PVSS row shading effects, the electricity generation efficiency of the subjacent PVSS row is significantly reduced. This has a significant impact on its comprehensive energy and economic performances for some regions. This paper uses a special PV module configuration which considers this shading effect. NEC, BC, and CB indicators were also employed to evaluate PVSS comprehensive energy and economic performances.

- The numerical shading model put forward in this paper accurately analyzes the shading effect from an upper PVSS row on its subjacent row and was used to investigate the detailed shading effect in various climatic regions.
- As for cities with similar latitudes to Harbin and Beijing, there is no shading effect from the upper PVSS row on its subjacent row. Considering the PVSS comprehensive energy and economic performances, the optimum tilt angles for Harbin and Beijing are 55°and 50°, respectively, while the optimum widths, in both cities, are all 1.156m.
- In terms of cities with similar latitudes to Changsha, Kunming, and Guangzhou, shading effect gets worse as latitude lowers. As tilt angle decreases, shading effect increases, which leads to variations in optimum tilt angles. In Changsha, Kunming, and Guangzhou, the optimum tilts are 40°, 40°, and 30°, respectively, with the optimum widths, for all, being 1.156m.
- PVSS with optimum widths and tilt angles in Harbin, Beijing, Changsha, Kunming and Guangzhou all show excellent comprehensive energy and economic performances compared with the rooftop PV systems and traditional electricity supply modes. PVSS is indicated as applicable for installation in multi-story buildings in these five climatic regions.

In this study, the comprehensive energy and economic performances of PVSS were comprehensively analyzed taking the shading effect into account. This would be valuable and helpful for building energy engineers and decision-makers to determine the design parameters of PVSS in different locations, and therefore promote the building energy efficiency. As for the numerical shading model, nearby shading objects were not considered. More precise numerical shading models considering nearby shading objects still need to be improved as it can better reflect the shading effect with considering the surrounding conditions. Finally, a more comprehensive sensitivity analysis and LCC analysis needs to be further conducted to provide a better understanding of the energy and economic performance of applying PVSS system.

Acknowledgements

This research was supported by the National Natural Science Foundation of China (Project No. 51608185), the Collaborative Innovation Center of Building Energy Conservation & Environmental Control, the Fundamental Research Funds for the Central Universities (Hunan University) and the Shenzhen Peacock Plan (KQTD2015071616442225).

References

[1] Shen JC, Zhang XX, Yang T, Tang L, Shinohara H, Wu YP, Wang H, Pan S, Wu JS, Xu P. Optimizing the Configuration of a Compact Thermal Façade Module for Solar Renovation ConNECt in Buildings. Energy Procedia 2016; 104: 9-14.
[2] BERC (Building Energy Research Center, Tsinghua University). Annual report on the development of building energy saving in China 2017. Building energy research center, Beijing, China, 2017.

[3] Peng JQ, Lu L, Yang HX. An experimental study of the thermal performance of a novel photovoltaic double skin façade in Hong Kong. Solar Energy 2013; 97: 293-304.
[4] Peng JQ, Lu L, Yang HX, Ma T. Comparative study of the thermal and power performances of a semi-transparent photovoltaic façade under different ventilation modes. Applied Energy 2015; 138: 572-583.
[5] Peng JQ, Curcija DC, Lu L, Selkowitz SE, Yang HX, Zhang WL. Numerical investigation of the energy saving potential of a semi-transparent photovoltaic double-skin façade in a cool summer Mediterranean climate. Applied Energy 2016; 165: 345-356.
[6] Peng JQ, Lu L, Yang HX, Han J. Investigation on the annual thermal performance of a PV wall mounted on a multi-layer façade. Applied Energy 2013; 112: 646-656.
[7] Wang M, Peng JQ, Li NP, Yang HX, Wang CL, Li X, Lu T. Comparison of energy performance between PV double skin façades and PV insulating glass units. Applied Energy 2017; 194: 148-160.
[8] Wang M, Peng JQ, Li NP, Lu L, Ma T, Yang HX. Assessment of energy performance of semi-transparent PV insulating glass units using a validated simulation model. Energy 2016; 112: 538-548.
[9] Park HS, Koo C, Hong T, Oh J, Jeong K. A finite element model for estimating the techno-economic performance of the building-integrated PV blind. Applied Energy 2016; 179: 211-227.
[10] Hong T, Koo C, Jeong K, Oh J, Jeong K. Nonlinearity analysis of the shading effect on the technical–economic performance of the building-integrated PV blind. Applied Energy 2017; 194: 467-480.
[11] Koo C, Hong T, Jeong K, Ban C, Oh J. Development of the smart PV system blind and its impact on net-zero energy solar buildings using technical-economic-political analyses. Energy 2017; 124: 382-396.
[12] Yanyi S, Katie S, Hasan B, Wei Z, Xia H, Yongxue L, Bo H, Robin W, Hao L, Senthilarasu S, Jingquan Z, Lingzhi X, Tapas M, Yupeng W. Integrated semi-transparent cadmium telluride photovoltaic glazing into windows: Energy and daylight performance for different architecture designs. Applied Energy 2018; 231: 972-984.
[13] Yuanda C, Min G, Jie J, Yanyi S, Yi F, Min Y. An optimal and comparison study on daylight and overall energy performance of double-glazed photovoltaics windows in cold region of China. Energy 2019; 170: 356-366.
[14] Li Y, Liu CL. Techno-economic analysis for constructing solar PV projects on building envelopes. Building and Environment 2018; 127: 37-46.
[15] Norton B, Eames PC, Mallick TK, Huang MJ, McCormack SJ, Mondol JD. Enhancing the performance of building integrated PVs, Solar Energy 2011; 85: 1629-1664.
[16] Sun LL, Yang HX. Impacts of the shading-type building-integrated PV claddings on electricity generation and cooling load component through shaded windows. Energy and Buildings 2010; 42 (4): 455-460.
[17] Sun LL, Lu L, Yang HX. Optimum design of shading-type building-integrated

PV claddings with different surface azimuth angles, Applied Energy 2012; 90: 233-240.
[18] Sun LL, Hu W. Dynamic performance of the shading-type building-Integrated PV claddings, Procedia Engineering 2015; 121: 930-937.
[19] Yoo SH, Lee ET. Efficiency characteristic of building integrated PVs as a shading device, Build Environment 2001; 37: 615-623.
[20] Yoo SH, Manz H. Available remodeling simulation for a BIPV as a shading device, Solar Energy Mater Solar Cells 2011; 95: 394-397.
[21] Hu JP, Rao ZH, Liao SM. Energy conservation for building integrated with PV shading system, New Energy & Green Building 2012; 40: 33-37.
[22] Hu JP. Optimization design and energy performance research for building integrated with PV shading system. Changsha: Central South University, 2012.
[23] Zhang WL, Lu L, Peng JQ. Evaluation of potential benefits of solar PV shadings in Hong Kong. Energy 2017; 137: 1152-1158.
[24] EnergyPlus. EnergyPlus 8.5. Washington DC, USA: US Department of Energy; 2016.
[25] Bingol O, Ozkaya B. Analysis and comparison of different PV array configurations under partial shading conditions. Solar Energy 2018; 160: 336-343.
[26] Reisi AR, Moradi MH, Jamasb S. Classification and comparison of maximum power point tracking techniques for PV system: a review, Renewable and Sustainable Energy Reviews 2013; 19: 433-443.
[27] Subudhi B, Pradhan R. A comparative study on maximum power point tracking techniques for PV power systems. IEEE Transactions on Sustainable Energy 2012; 4(1): 89-98.
[28] Bhatnagar P, Nema RK. Maximum power point tracking control techniques: state-of-the-art in PV applications. Renewable and Sustainable Energy Reviews 2013; 23: 224-241.
[29] Malathy S, Ramaprabha R. Comprehensive analysis on the role of array size and configuration on energy yield of PV systems under shaded conditions. Renewable and Sustainable Energy Reviews 2015; 49: 672-679.
[30] Eltawil MA, Zhao Z. MPPT techniques for PV applications. Renewable and Sustainable Energy Reviews 2013; 25: 793-813.
[31] Verma D, Nema S, Shandilya AM, Dash SK. Maximum power point tracking (MPPT) topology: recapitulation in solar PV systems. Renewable and Sustainable Energy Review 2014; 54: 1018-1034.
[32] Pendem SR, Mikkili S. Modelling and performance assessment of PV array topologies under partial shading conditions to mitigate the mismatching power losses. Solar Energy 2018; 160: 303-321.
[33] Yadav AS, Pachauri RK, Chauhan YK, Choudhury S, Singh R. Performance enhancement of partially shaded PV array using novel shade dispersion effect on magic-square puzzle configuration. Solar Energy 2017; 144: 780-797.
[34] Yadav AS, Pachauri RK, Chauhan YK. Comprehensive investigation of PV arrays with puzzle shade dispersion for improved performance. Solar Energy 2016; 129: 256-285.

[35] Mahammed IH, Arab AH, Berrah S, Bakelli Y, Khennene M, Oudjana SH, Fezzani A, Zaghba L. Outdoor study of partial shading effects on different PV modules technologies. Energy Procedia 2017; 141: 81-85.
[36] Malathy S, Ramaprabha R. Reconfiguration strategies to extract maximum power from PV array under partially shaded conditions. Renewable and Sustainable Energy Reviews 2018; 81: 2922-2934.
[37] Wu LL, Wang YH, Cheli GE, Wang JJ, Tian R. Experimental study of partial shadow effect on PV system. Chinese Journal of Power Sources 2016; 40: 774-776.
[38] Duffie J, Beckman W. Solar engineering of thermal processes. 1980, p13-20.
[39] Cooper PI. The absorption of radiation in solar stills. Solar energy 1969; 12(3): 333-346.
[40] Braun JE. Mitchell JC. Solar geometry for fixed and tracking surfaces solar energy 1983; 31(5):439-444.
[41] NREL. NREL System Advisor Model (SAM). [Online] 21 7 2016. <https: //sam.nrel.gov/>.
[42] Construction, M.o. and I.a.Q. General Administration of Quality Supervision, GB50189-2015 Design Standard for Energy Efficiency of Public Buildings, Ministry of Construction, 2015.
[43] Peng JQ, Lu L, Yang HX, Ma T. Validation of the Sandia model with indoor and outdoor measurements for semi-transparent amorphous silicon PV modules. Renewable Energy 2015; 80: 316-323.
[44] Markvart T. Solar electricity. NewYork, USA: John Wiley&Sons; 1994.
[45] Messenger R, Ventre J. Photovoltaic systems engineering. BocaRaton, Florida, USA: CRC Press LLC; 2000.
[46] Celik AN. Effect of different load profiles on the loss-of-load probability of stand-alone photovoltaic systems. Renewable Energy 2007; 32: 2096-2115.
[47] Ajan CW, Ahmed SS, Ahmed HB, Taha F, Zin AABM. On the policy of photovoltaic and diesel generation mix for an off grid site: East Malaysian Perspectives. Sol Energy 2003; 74: 453-467.
[48] Celik AN. Present status of photovoltaic energy in turkey and life cycle techno-economic analysis of a grid-connected photovoltaic house. Renewable Sustainable Energy Rev 2006; 10:370-387.
[49] Abdul G, Anjum M. Design and economics analysis of an off-grid PV system for household electrification. Renewable Sustainable Energy Rev 2015; 42:496-502.
[50] Kamalapur G, Udaykumar R. Rural electrification in India and feasibility of photovoltaic solar home systems. Int J Electr Power Energy Syst 2011; 33 (3):594-599.
[51] Shaahid S, Elhadidy M. Economic analysis of hybrid photovoltaic-diesel battery power systems for residential loads in hot regions—a step to clean future. Renewable Sustainable Energy Rev 2008; 12: 488-503.
[52] Ajao KR, Ajimotokana HA, Popoolaa OT, Akande HF. Electric energy supply in Nigeria, decentralized energy approach. Cogeneration Distrib Gener J 2009; 24 (4): 34-50.
[53] He YX, Pang YX, Li XM, Zhang MH. Dynamic subsidy model of PV distributed

generation in China. Renewable Energy 2018; 118: 555-564.
[54] Raman V, Tiwari GN. Life cycle cost analysis of HPVT air collector under different Indian climatic conditions. Energy Policy 2008; 36: 603-611.
[55] Burhenne S, Tsvetkova O, Jacob D, Henze GP, Wagner A. Uncertainty quantification for combined building performance and cost-benefit analyses. Build Environ 2013; 62: 143-154.
[56] Wang N, Chang Y-C, El-Sheikh A. Monte Carlo simulation approach to life cycle cost management. Struct Infrastruct Eng 2012; 8: 739-746.
[57] Das P, Van Gelder L, Janssen H, Roels S. Designing uncertain optimization schemes for the economic assessment of stock energy-efficiency measures. J Build Perform Simul 2015; 1493: 1-14.
[58] Rahman S, Vanier DJ. Life cycle cost analysis as a decision support tool for managing municipal infrastructure. CIB 2004 Triennial Congress. Toronto, Ontario; 2004. p. 1-12.